



CHORUS

This is the accepted manuscript made available via CHORUS. The article has been published as:

Origin of Transitions between Metallic and Insulating States in Simple Metals

Ivan I. Naumov and Russell J. Hemley

Phys. Rev. Lett. **114**, 156403 — Published 17 April 2015

DOI: [10.1103/PhysRevLett.114.156403](https://doi.org/10.1103/PhysRevLett.114.156403)

Origin of transitions between metallic and insulating states in simple metals

Ivan I. Naumov[‡] and Russell J. Hemley^{‡*}

*Geophysical Laboratory, Carnegie Institution of Washington,
5251 Broad Branch Road NW, Washington DC 20015, USA*

Unifying principles that underlie recently discovered transitions between metallic and insulating states in elemental solids under pressure are developed. Using group theory arguments and first-principles calculations, we show that the electronic properties of the phases involved in these transitions are controlled by symmetry principles not previously recognized. The valence bands in these systems are described by simple and composite band representations constructed from localized Wannier functions centered on points *unoccupied* by atoms, and which are not necessarily all *symmetrical*. The character of the Wannier functions is closely related to the degree of *s-p(-d)* hybridization and reflects multi-center chemical bonding in these insulating states. The conditions under which an insulating state is allowed for structures having an integer number of atoms per primitive unit cell as well as re-entrant (*i.e.*, metal-insulator-metal) transition sequences are detailed, resulting in predictions of novel behavior such as phases having three-dimensional Dirac-like points. The general principles developed are tested and applied to the alkali and alkaline earth metals, including elements where high-pressure insulating phases have been identified or reported (*e.g.*, Li, Na, and Ca).

When atoms are brought together, their electronic wave functions overlap and hybridize, and one should expect a sudden transition from an insulating to a metal state at some critical interatomic spacing. This scenario is the essence of a classic Mott insulator-metal transition induced by pressure [1]. It is reasonable to expect, and has long been assumed, that once converted into a metal the system will remain in this state upon further compression. In reality, however, all the alkali metals and heavy alkaline earth metals (Ca, Sr and Ba), do not follow this anticipated behavior; rather they become progressively less conductive on compression, at least up to some critical limit over a broad pressure range. Of these metals, Li and Na clearly undergo pressure-induced metal-insulator transitions, which may also be called reverse Mott transitions. According to direct electrical resistance measurements, Li becomes semiconducting near 80 GPa [2], and reverts to a metallic state above 120 GPa [3], while Na enters a wide-gap insulating state above 180 GPa becoming transparent to visible light [4]. *fcc*-Ca is also believed to undergo a metal-insulator (semiconductor) transition (at ~ 19 GPa) before transforming to the metallic *bcc* phase, based on electrical resistivity measurements [5, 6] and subsequent theoretical calculations that predict a small band gap (~ 0.1 eV) at these compressions [7]. Moreover, at ultrahigh pressures (34 TPa), it is also predicted that Ni passes through an insulating state [8].

High-pressure studies have established that metals can lose electrical conductivity either continuously within a given phase or abruptly when undergoing a structural transformation. In the “continuous” regime, these changes have been variously attributed to *s-p* (Li, Na), *p-d* (Na) or *s-d* (K, Cs, Rb, Ca, Sr, Ba) electronic transitions accompanied by the movement of valence electrons from the atoms to interstitial sites in the structure [4, 9-16]. However, there is disagreement on the extent and nature of hybridization, how the mixing is related to interstitial electronic localization, how such localization is related to the metal-insulator transition, and the conditions under which the material returns to a metallic state at higher pressure. The “abrupt” drops in conductivity at structural transformations, on the other hand, have been interpreted as the result of Peierls distortions [17] or the formation of Hume-Rothery phases in which parts of the Fermi surface disappear due to contact with the Brillouin zone (BZ) boundaries [18]. However, these two mechanisms cannot explain (or predict) complete “dielectrization” of the electronic spectrum in these metals. Indeed, Peierls distortions in three-dimensional metallic systems are capable of opening a gap only over the limited flat patches of the initial Fermi surface separated by some (nesting) vector $2\mathbf{k}_F$ [19]. As for the Hume-Rothery model, this

condition requires the phases to be highly symmetric structures in order for the BZ planes to tightly envelop the Fermi surface [20, 21]; on the other hand, the observed high-pressure insulating structures (*e.g.*, Li and Na) are significantly anisotropic and not of the Hume-Rothery type.

Here we develop a unified framework for understanding transitions between metallic and insulating states of simple metals on compression. Since such metals are only weakly correlated systems [22, 23], the problem was treated within a standard one-electron band theory. Using the concept of localized Wannier functions (WFs) and group theory arguments, we detail the conditions under which insulating states are allowed for structures having an integer number of atoms per primitive unit cell. Further, from first-principles calculations on real and model systems we demonstrate the connection between orbital mixing, redistribution of electronic charge from the nucleus to the periphery, and the opening of the band gap. We show that *s-p* mixing is responsible for opening up a global band gap in simple metals to form an insulating state in the systems examined to date. Moreover, the symmetry principles developed here allow generalizations that lead to specific predictions for metal-insulator, as well as re-entrant insulator-metal transitions, for other systems. The approach demonstrates, for example, that a finite band gap in Ca cannot exist in the *fcc* structure but instead enters a topological semimetallic state characterized by three-dimensional Dirac-like points [24].

It is well known that Bloch valence states in systems of non-interacting electrons with a band gap can always be described by localized WFs (with finite spread) [25-27]. The number of WFs must be equal to the number of occupied valence band branches, J , and at the same time equal to the sum $\sum_i n_w^i d_i$, where the index i is used to distinguish between different sets of WFs (or band representations [28]), n_w^i is the multiplicity of a Wyckoff position associated with the centers of the WFs belonging to set i , and d_i is the dimension of an irreducible representation (*irrep*) describing the point symmetry of this position. In non-symmorphic structures, n_w^i are always ≥ 2 as are the corresponding numbers of WFs. In the *hcp* structure, for example, all the WFs can be grouped in pairs such that any WF from a pair can be obtained from its counterpart by applying a screw axis operation ($C_2|c/2$). It is therefore impossible to isolate a single Bloch branch in this case, which would require that all the alkali metals (including hydrogen) in the *hcp*

phase to be (semi)metallic despite the presence of two electrons per primitive unit cell or integer band filling, $n=1$ [29].

With two atoms per cell and being non-symmorphic, the diamond structure (space group $Fd-3m$) exhibits behavior similar to the *hcp* arrangement. The symmetry centers (Wyckoff positions) in this structure have at least two vectors in the star [30], which precludes the splitting off of a single-sheeted band. As a result, all alkali metals crystallizing in the diamond structure would be (semi)metallic, analogous to the system described above. In this context, it is useful to consider the Hume-Rothery phase *cI16* ($I-43d$) found experimentally in compressed Li and Na [18]. Like the classic γ -brass system, Li-*cI16* exhibits a small density of states at E_F and low reflectivity, and might be expected to transform into an insulator at higher pressures. This possibility, however, is symmetrically forbidden because the minimal multiplicity of Wyckoff positions in *cI16* is 6, and it is impossible to construct a four-branched band accommodating 8 valence electrons (per primitive unit cell). It should be stressed that even fulfilling the condition $J = \sum_i n_w^i d_i$ may not be sufficient for the corresponding system to reach an insulating state. This is the case of *fcc*-Ca, as we show below.

We now proceed to the insulating phases found experimentally in Li and Na under pressure. Insulating Na has a band gap of 1.3 eV near 200 GPa and adopts a double hexagonal close packed structure (*hP4*, space group $P6_3/mmc$, see Ref. [22]) with Na atoms occupying Wyckoff positions $2a$ (0,0,0) and $2d$ ($2/3, 1/3, 1/4$) [4]. The corresponding phase in Li has a smaller energy gap (~ 1 eV at 90 GPa) and a more complicated, non-centrosymmetric crystal structure with space group *Aba2* where five nonequivalent Li atoms occupy $8b$ (x,y,z) sites (40 and 20 atoms per conventional and primitive unit cells, respectively) [31, 32]. According to Ref. [4], the insulating state in *hP4*-Na arises from localization of valence electrons in the interstitial sites enabled by *p-d* hybridization. This proposal can be examined by replacing the Na atoms in the structure with Li and analyzing how the electronic structure changes. We find that *hP4*-Li also has an appreciable band gap at these compressions, despite the fact that the *p-d* hybridization effects are negligible (Fig. 1). Moreover, the valence electrons in *hP4*-Li localize in the interstitial regions, and their distribution is very similar to that in *hP4*-Na. The maxima locate at $2c$ ($1/3, 2/3, 1/4$) Wyckoff positions where the crystal potential is maximal. Such an

unusual situation reflects the tendency of electrons to reduce their kinetic energy by occupying the more open interstitial regions, as discussed for the classic electride $\text{Cs}^+(15\text{-crown})_2\text{e}^-$ [33].

We now show how group theory arguments and WFs can be used to characterize these systems. In *hP4*-Na, the valence band consisting of two branches splits off from the rest of the band structure, thereby opening a band gap. The fact that the centers of valence electronic charge coincide with the *unoccupied* $2c$ (1/3,2/3,1/4) Wyckoff positions means that the valence band can be described by the single set of localized WFs centered exactly on that position [28, 34]. Since $J=2$ and $n_w=2$, the dimension of an *irrep* should be equal to 1. Since the band under discussion is bonding in character, we represent it with fully symmetric WFs, and the correct one-dimensional *irrep* is A_1 [22]. This assumption can be easily checked by examining the Wannier basis (c, A_1) which leads to two Bloch states at Γ (Γ_1^+ , and Γ_4^-) that are invariant with respect to all the elements that comprise the point group of the sites $2c$. The calculated wave functions corresponding to the Γ_1^+ , and Γ_4^- levels are both completely bonding in the (x,y) -plane (Fig. 2). At high isosurfaces (*e.g.*, ~ 2.5), the bottom valence band wave function Γ_1^+ (Fig. 2a) represents a bonding combination of purely *s*-like orbitals centered on all the Na atoms. Similarly, at high isosurfaces the top valence band wave function Γ_4^- represents a symmetrical combination of *s-d_{z²}* hybrids centered on the Na2 atoms (Figs. 2c; see also Ref. [22]). The *d* (or even *f*) character of this band can also be found in other \mathbf{k} -regions of the BZ. Thus, even though the top valence band is mainly of *s-p* character, it also contains a significant *d* component ($\sim 20\%$) in particular regions of reciprocal space. This is quite natural: the Bloch functions can possess any orbital character because they are expressed in terms of WFs and projected on spherical harmonics around the atomic sites.

The situation becomes more interesting and complex for insulating Li. In the *Aba2* structure Li exhibits three distinct maxima in the electron density in the interstitial region [22]. All the maxima are located on $8b$ sites, but only two of them, $M1$ and $M2$, can be viewed as the centers of the “pseudoanions” holding roughly 2 electrons [32]. At the same time, the integrated density within the $M3$ attractors gives only 1 electron. Since in a non-spin-polarized system each localized WF (when squared and integrated) should give 2 electrons, *only* the $M1$ and $M2$ maxima can be identified as the centers of such functions, \mathbf{r}_1 and \mathbf{r}_2 ($\mathbf{r}_1 = M1$, $\mathbf{r}_2 = M2$). At the same time two neighboring $M3$ maxima, $M3$ and $M3$, should be viewed as signatures of

one WF centered exactly between them: $\mathbf{r}_3=(M3\Box+M3\Box\Box)/2$. From this, we can construct a band representation describing a ten-branched valence band [22]. In contrast to *hP4*, the band representation in *Aba2* is *composite* [35], and consists of three simple band representations $(a, A)^+ (b, A)^+ (b, A)$. Our calculations show that 10 WFs forming a basis of the representation $(a, A)^+ (b, A)^+ (b, A)$ reproduce the ten-branched band of *Aba2*-Li perfectly. Moreover, we find that the maximally localized WF approach, with (initially) randomly-centered Gaussian functions, leads practically to the same centers that identified above using solely information about the valence charge distribution in the interstitial regions presented in Ref. [32]. The spread in WFs is significant, which explains why the *M1*, *M2* and *M3* charge maxima merge into a single super-basin [32]. The offset in positions of the WFs in Li gives rise to the prediction of a remarkably large macroscopic electrical polarization in its high-pressure insulating state [22]. Interestingly, in *Aba2*-Li, in contrast to *hP4*-Na, the bottom and top valence band wave functions at Γ are centered in the voids even at high isosurfaces (*cf.* Figs. 2 and 3).

Moving to Ca, we find that under pressure the valence charge density in its *fcc* structure is concentrated in the interstitial region as in Li and Na, and forms four-leafed rosettes around the nuclei and smooth maxima centered on the octahedral Wyckoff positions (Fig. 4). Despite this shift in charge, the system does not open up a gap in this structure, in contrast to recent claims. We find that the phase cannot be properly described using one set of WFs centered on the octahedral positions because the first and second branches touch each other along *L-W*. In fact, there are 24 such isolated points of contact over the whole BZ which gives rise to a series of Dirac-like points. These Dirac-like points are not required by symmetry but nevertheless cannot be destroyed or broken by infinitesimal changes in the lattice parameter [36]. The physical reason is that the state at *L* just above E_F is pure $4p$, and moves up with the pressure, whereas the same the state at *W* just below the E_F is mainly of $3d$ character and moves down. Thus, the valence and conduction bands between *L* and *W* move like a scissors operator to form a series of Dirac-like points. We also point out that eliminating the *d*-component from *s-p-d* hybridization along *L-W* allows the system to open a gap, as demonstrated by numerical calculations for *fcc* Ca over a range of lattice parameters (*i.e.*, including negative pressures).

This approach shows that it is the *s-p* electronic transition that drives these metals into insulating states. The interconnection between the *s-p* electronic transition, development of

interstitial charge, and “dielectrization” can be understood from a simple model systems such as a one-dimensional crystal of Li and Na. Both analytical tight-binding and explicit numerical calculations for this hypothetical system reproduce the essential features of the s - p electronic transition in real Li or Na [22]. Notably, we find that there are two types of s - p hybridization that are equally important for opening the band gap. The first corresponds to the mixing of s and $p_x(p_y)$ orbitals at the same lattice sites, as exemplified by $hP4$ -Na. This mixing is the principal origin of the dielectrization of the spectrum along the \mathbf{k} -directions parallel to the basal plane. The second type of hybridization arises from the overlap of s and p_z (as well as d_{z^2}) orbitals at different lattice sites. This type is crucial for forming a band gap at Γ . The d contribution to the wave function is not necessary for gap opening; as we already have seen the gap still opens in passing from Na to Li in the $hP4$ structure. These insulating phases therefore exhibit multi-center s - p ($-d$) bonding. The WFs associated with such a bonding are centered *not* at midpoints of the lines joining neighboring atoms (as in common covalent crystals such as diamond) but rather in the voids separated more or less equally from several atoms. This multi-center bonding is directional as in conventional covalent systems but in contrast to that in metals.

We now compare the approach with previous work. Neaton and Ashcroft [17] first explicitly examined the pressure-induced change from s to p character of the bands in Li and the pairing distortion in Li. Our results indicate that development of a band gap in Li (as well as other alkali metals) is mainly due to strong s - p hybridization, though other types of hybridization (s - d , p - d , *etc.*) can facilitate the opening of a gap. In the case of $hP4$ -Na, we can distinctly see that both “vertical” s - p_z and “in-plane” s - $p_x(p_y)$ hybridizations are equally important. This contrasts with the view that the dielectrization process arises from s - p_z [14-16] or p - d [4] hybridization. The general approach developed here has parallels to the simple high-pressure electrone model developed by Miao and Hoffmann [37]. In the context of alkali metals, this model focuses on the relative position of the s orbital energy with respect to, not to p or d orbital energies but instead to the $1s$ energy associated with the so-called interstitial quasiatom (ISQ), an interstitial space that can be occupied by the electrons (*i.e.*, similar to the WFs used here). On the other hand, the simple ISQ model does not predict metallic re-entrant behavior as (*e.g.*, Li reverting to a metallic state above 120 GPa) in contrast to our approach where it appears naturally. In another approach, Degtyareva [18] used Hume-Rothery arguments to explain selected transitions in simple metals, such as the transformation to $cI16$ phase in Li. Though the

Hume-Rothery approach rationalizes the formation of a pseudogap at the Fermi level, it cannot predict which high-pressure phases are in fact insulating (*e.g.*, *cI16* discussed above). Finally, we note that the approach developed here has some parallels with generalized-valence-bond models for chemical bonding in alkali and noble metals [38]. We also point out that the transitions considered here for simple metals principally differ from that predicted at ultrahigh pressures for Ni [8] where the band gap closes not as a result of orbital mixing but due to the opposite process of the rise in 4s above the 3d .

In conclusion, use of localized WFs and group theory provides a framework for understanding the anomalous transitions between the metallic and insulating states of simple elements observed on compression. Insulating states are not automatically allowed for the structures having an integer number of atoms per primitive unit cell. The alkali metals, for example, cannot be insulating in non-symmorphic structures with a filling of 1, but only with integer fillings ≥ 2 . In Li and Na, the *s-s* antibonding states and *p-p* bonding states overlap to open hybridization gaps simultaneously at all BZ faces. At the same time, *s-d* or *s-p-d* electronic transitions do not lead to an insulating states, as in the case of *fcc* Ca whose valence energy band cannot be represented by a single set of WFs. This conclusion is also supported by the fact that the pressure-induced *s-d* transition in Cs (Cs-IV [39] and Cs-V [15]) does not open up a gap, even though it shifts the valence charge density from the nucleus to the interstitial region. High-pressure insulating states of simple “metals” occupy an intermediate place between metals and covalent crystals. The transitions between these states arise from the formation of flat *s-p* hybrid bands (and associated band gaps) near the Fermi level within a pressure window where the effective *s* and *p* energy levels are close to each other as well to E_F , a proximity that facilitates the observed re-entrant behavior. [40-43]

References

- [1] J. M. Ziman, *Principles of the Theory of Solids* (Cambridge University Press, Cambridge, 1979).
- [2] T. Matsuoka and K. Shimizu, *Nature* **458**, 186 (2009).
- [3] T. Matsuoka *et al.*, *Phys. Rev. B* **89**, 144103 (2014).
- [4] Y. Ma, M. Eremets, A. P. Oganov, Y. Xie, I. Trojan, S. Medvedev, A. O. Lyakhov, M. Valle, and V. Prakapenka, *Nature* **458**, 182 (2009).
- [5] K. J. Dunn and F. P. Bundy, *Phys. Rev. B* **24**, 1643 (1981).
- [6] R. A. Stager and H. G. Drickamer, *Phys. Rev.* **131**, 2524 (1963).
- [7] E. G. Maksimov, M. V. Magnitskaya, and V. E. Fortov, *Phys. Uspek.* **48**, 761 (2005).
- [8] A. K. McMahan and R. C. Alberts, *Phys. Rev. Lett.* **49**, 1198 (1982).
- [9] A. Bergara, J. B. Neaton, and N. W. Ashcroft, *Phys. Rev. B* **62**, 8494 (2000).
- [10] J. C. Boettger and S. B. Trickey, *Phys. Rev. B* **32**, 3391 (1985).
- [11] M. Hanfland, K. Syassen, N. E. Christensen, and D. L. Novikov, *Nature* **408**, 174 (2000).
- [12] A. Lazicki, A. F. Goncharov, V. V. Struzhkin, R. E. Cohen, Z. Liu, E. Gregoryanz, C. Guillaume, H. K. Mao, and R. J. Hemley, *Proc. Nat. Acad. Sci.* **106**, 6525 (2009).
- [13] J. B. Neaton and N. W. Ashcroft, *Phys. Rev. Lett.* **86**, 2830 (2001).
- [14] B. Rousseau, Y. Xie, Y. Ma, and A. Bergara, *Eur. Phys. J. B* **81**, 1 (2011).
- [15] U. Schwarz, O. Jepsen, and K. Syassen, *Sol. State. Comm.* **113**, 643 (2000).
- [16] R. Rousseau, K. Uehara, D. D. Klug, and J. S. Tse, *ChemPhysChem* **6**, 1703 (2005).
- [17] J. B. Neaton and N. W. Ashcroft, *Nature* **400**, 141 (1999).
- [18] V. F. Degtyareva, *High Press. Res.* **30**, 343 (2010).
- [19] M. I. Katsnelson, I. I. Naumov, and A. V. Triefilov, *Phase Trans.* **49**, 143 (1993).
- [20] M. L. Cohen and V. Heine, in *Solid State Physics: Advances and Applications*, edited by H. Ehrenreich, F. Seitz, and D. Turnbull (Academic Press, New York, 1970), pp. 37.
- [21] V. Heine and D. Weaire, in *Solid State Physics: Advances and Applications*, edited by H. Ehrenreich, F. Seitz, and D. Turnbull (Academic Press, New York, 1970), p. 250.
- [22] See Supplemental Materials on [http:// www.aip.org/pubservs/epaps.html](http://www.aip.org/pubservs/epaps.html), which contains Refs. [40-43].
- [23] A. Heilingbrunner and G. Stolhoff, *J. Chem. Phys.* **99**, 6799 (1993).
- [24] Semimetallic phases have either a zero-band gap or very small overlap between the valence or conduction bands resulting in a negligible density of states at the Fermi level, and thus occupy an intermediate niche between metallic and insulating.
- [25] N. Marzari, A. A. Mostofi, J. R. Yates, I. Souza, and D. Vanderbilt, *Rev. Mod. Phys.* **84**, 1419 (2012).
- [26] R. Resta, in *Fundamental Physics of Ferroelectrics 2000* (2000).
- [27] I. Souza, T. Wilkens, and R. M. Martin, *Phys. Rev. B* **62**, 1666 (2000).
- [28] J. Zak, *Phys. Rev. B* **23**, 2824 (1981).
- [29] This property is closely related to the fact that the energy branches in hcp structures always stick together in pairs over the entire symmetry planes perpendicular to c (π/c and $-\pi/c$) due to time-inversion symmetry [26]. The filling of the electronic bands, n , is defined as one-half the number of valence electrons per primitive unit cell.
- [30] J. Zak, *Phys. Rev. Lett.* **62**, 2747 (1989).
- [31] J. Lv, Y. Wang, L. Zhu, and Y. Ma, *Phys. Rev. Lett.* **106**, 015503 (2011).
- [32] M. Marques, M. I. McMahon, E. Gregoryanz, M. Hanfland, C. Guillaume, C. J. Pickard, G. J. Ackland, and R. J. Nelmes, *Phys. Rev. Lett.* **106**, 095502 (2011).
- [33] D. J. Singh, H. Krakauer, C. Hass, and W. E. Pickett, *Nature* **365**, 39 (1993).
- [34] J. Des Cloizeaux, *Phys. Rev.* **129**, 554 (1963).

- [35] R. A. Evarestov and V. P. Smirnov, *Site Symmetry in Crystals. Theory and Applications, 2nd ed.*, (Springer-Verlag, Berlin Heidelberg New York, 1997), Vol. 108.
- [36] C. Herring, Phys. Rev. **52**, 365 (1937).
- [37] M. S. Miao and R. Hoffmann, Acc. Chem. Res. **47**, 1311 (2014).
- [38] M. H. McAdon and W. A. Goddard III, Phys. Rev. Lett. **55**, 2563 (1985).
- [39] E. Zurek, O. Jepsen, and O. K. Andersen, ChemPhysChem **6**, 1934 (2005).
- [40] J. K. Burdett, *Chemical Bonding in Solids (Topics in Inorganic Chemistry)* (Oxford University Press, Oxford, 1995).
- [41] M. Imada, A. Fujimori, and Y. Rokura, Rev. Mod. Phys. **70**, 1039 (1998).
- [42] M. B. Lepetit, E. Apra, J. P. Malrieu, and R. Dovesi, Phys. Rev. B **46**, 12974 (1992).
- [43] L. Michel and J. Zak, Europhys. Lett. **18**, 239 (1992).

Figures

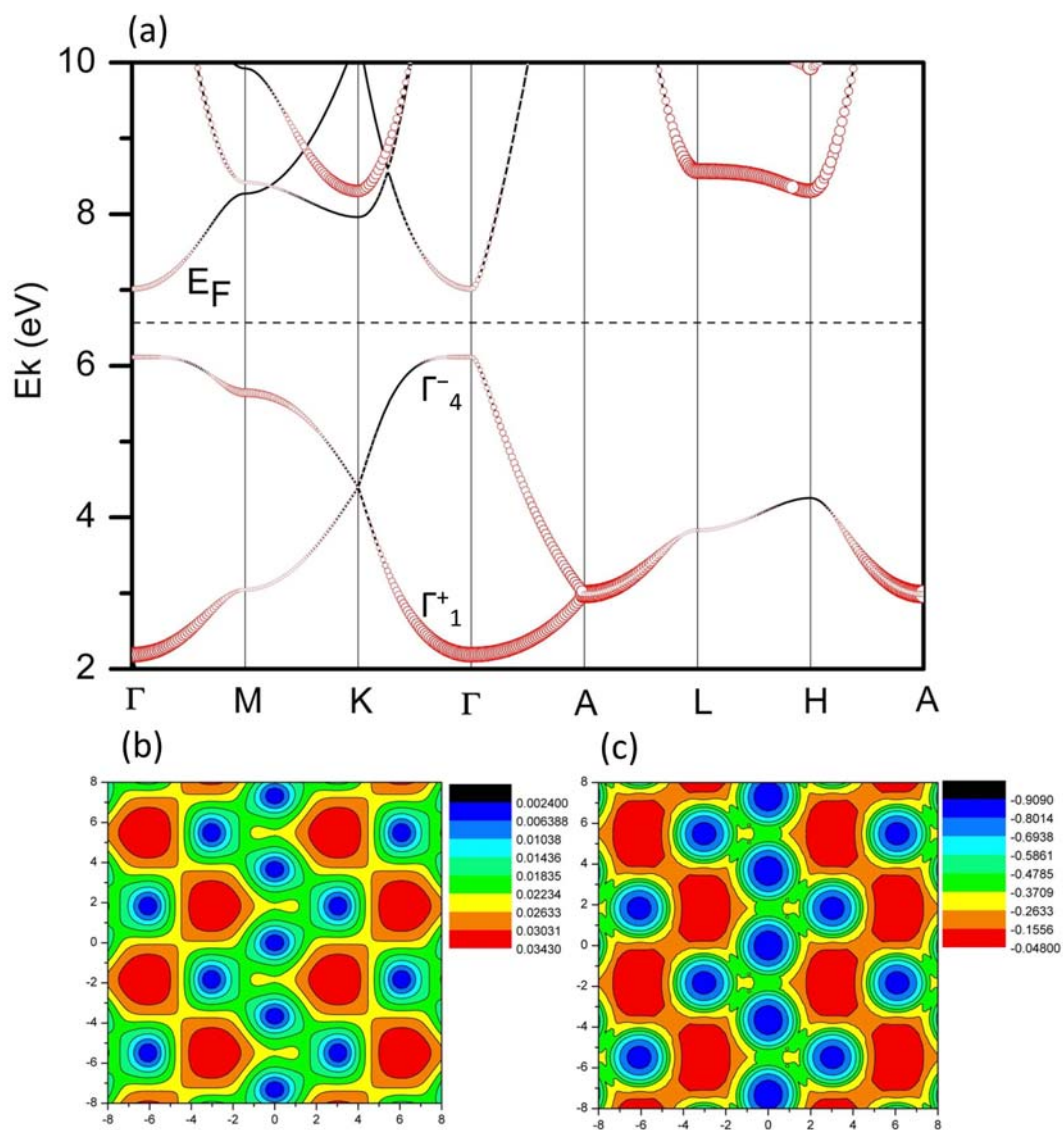


Figure 1. Electronic properties of *hP4*-Li for lattice parameters $a=2.784 \text{ \AA}$, $c=3.873 \text{ \AA}$ (90 GPa). The parameters are intentionally kept the same as for *hP4*-Na at 320 GPa. (a) Band structure; the size of red circles is proportional to the s character of the Bloch wave functions. (b,c) Valence charge density and crystal potential in the (110) plane, respectively. The ions are centered in the blue regions.

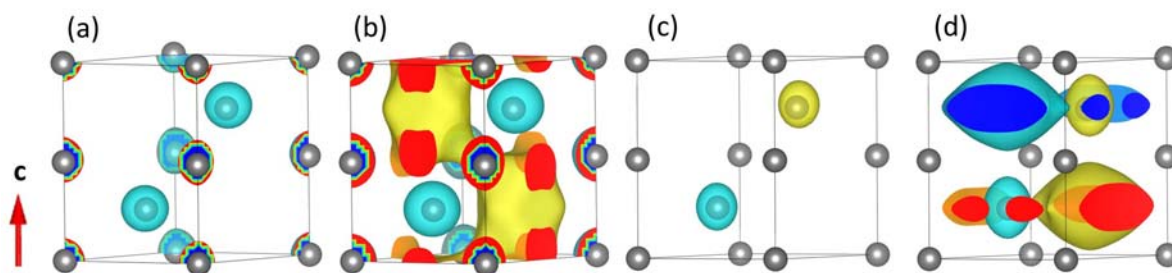


Figure 2. Bottom and top valence band wave functions at Γ in *hP4*-Na at 320 GPa (corresponding to Γ_1^+ and Γ_4^- energy levels) in the primitive unit cell. (a, b) Isocontours of Γ_1^+ at ± 2.5 and ± 1.1 , respectively (yellow for + and light blue for -). (c, d) Same as (a, b) but for Γ_4^- .

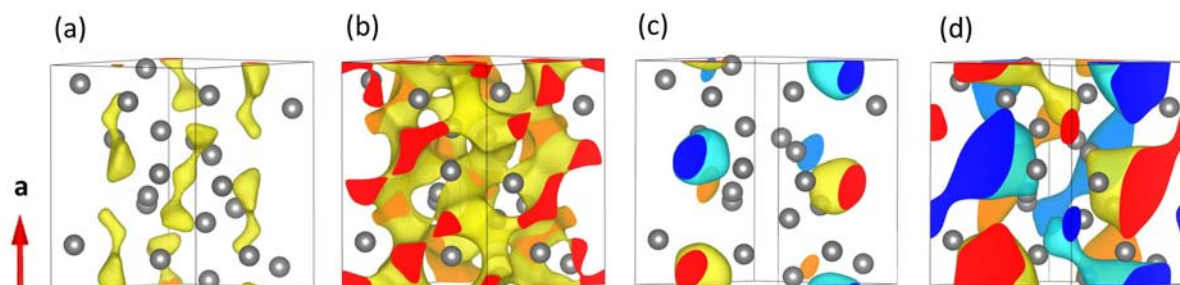


Figure 3. Bottom and top valence band wave functions at Γ in *Aba2*-Li at 80 GPa in the primitive unit cell. (a, b) Isocontours of the bottom wave function at ± 1.2 and ± 1.1 , respectively. (c, d) Same as (a, b) but for the top wave function at ± 1.8 and ± 1.2 .

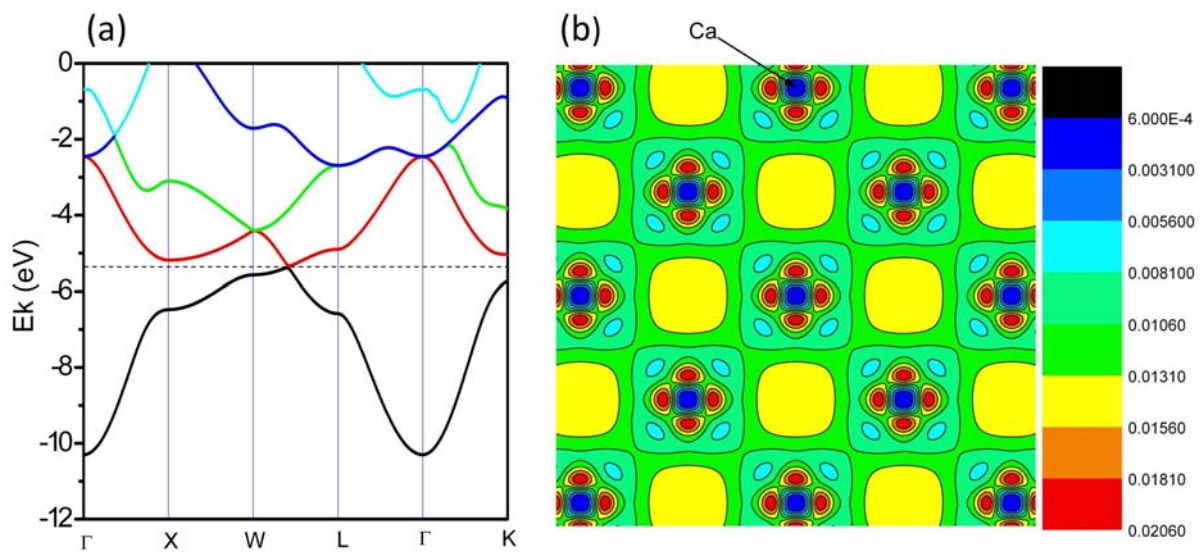


Figure 4. Electronic properties of *fcc* Ca at $a=4.706 \text{ \AA}$ and 19.0 GPa. (a) Band structure. (b) Valence charge density in the (100) planes passing through the Ca atoms (electrons/Bohr³).